Supplementary Material

Crystal contact engineering for enhanced cross-linking efficiency of HheG crystals

Marcel Staar[a], Sophie Staar[a], Anett Schallmey*[a,b,c]

[a] M. Staar, S. Staar, Prof. A. Schallmey
Institute for Biochemistry, Biotechnology and Bioinformatics
Technische Universität Braunschweig
Spielmannstr.7, 38106 Braunschweig (Germany)

[b] Prof. A. Schallmey
Zentrum für Pharmaverfahrenstechnik (PVZ)
Technische Universität Braunschweig
Franz-Liszt-Str.35a, 38106Braunschweig (Germany)

[c] Prof. A. Schallmey
Braunschweig Integrated Center of Systems Biology (BRICS)
Technische Universität Braunschweig
Rebenring 56, 38106 Braunschweig (Germany)

*Correspondence Author: Prof. A. Schallmey
E-mail: a.schallmey@tu-braunschweig.de
Hompage: https://www.tu-braunschweig.de/en/bbt/biochem

Additional tables and figures

Activity tests

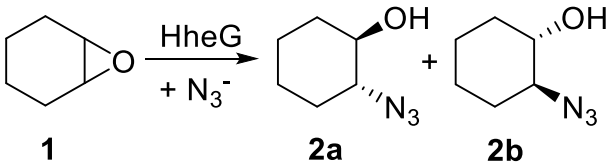

Scheme S1. Epoxide ring opening of cyclohexene oxide (**1**) catalyzed by HheG wild type and its variants using azide as nucleophile [**2a:** (1*R*,2*R*)-2-azido-1-cyclohexanol, **2b:** (1*S*,2*S*)-2-azido-1-cyclohexanol].

Crystal contact analysis

Table S1. Distances of natural lysines as well as residues selected for mutagenesis within the crystal contact of wild-type HheG.

Position	Residue	Distance C_α [Å]	Distance $-NH_2$ [Å]	Crystal contact
108	Lysine	25.6	15	tangential
119	Lysine	15.1	9.5	axial
121	Lysine	18.5	14	axial
205	Lysine	19.1	17.6	tangential
46	Valine	14.3	-	axial
115	Aspartic acid	11.9	-	axial
141	Alanine	11.7	-	tangential
185	Asparagine	12.8	-	tangential
217	Alanine	9.7	-	tangential

Crystallization

Table S2. Crystallization characteristics of different HheG variants based on crystallization in 2 µL scale.

Enzyme	Crystalli-zability rate[a] [%]	Crystalli-zation time[b] [h]	Minimal PEG concentration [%]	Minimal protein concentration [mg/mL]	Best crystallization conditions
WT	17.4	44	8	2	24 mg/mL proteinsolution; 10 mM HEPES, pH 7.0, 12% (w/v) PEG4000
V46K	49.3	4	2	6	24 mg/mL proteinsolution 10 mM HEPES, pH 7.3, 6% (w/v) PEG4000
D115K	0	-	-	-	-
A141K	62.5	4	2	6	24 mg/mL proteinsolution 10 mM HEPES, pH 7.3, 8% (w/v) PEG4000
R185K	38.2	20	10	18	24 mg/mL proteinsolution 10 mM HEPES, pH 7.3, 12% (w/v) PEG4000
A217K	0	-	-	-	-

[a] Calculated based on the number of wells with crystals devided by the total number of wells.
[b] Based on crystallization in 20 µL scale.

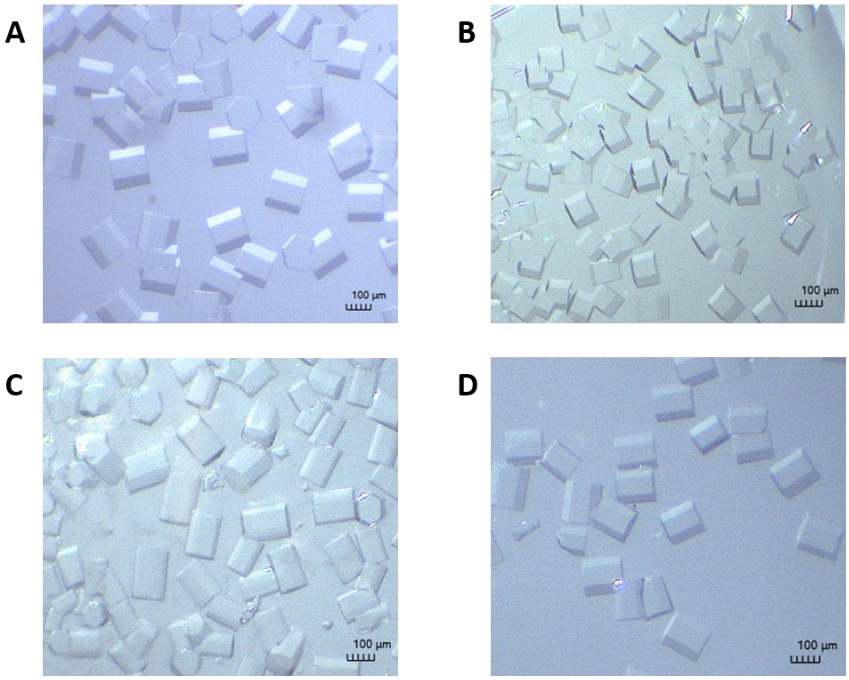

Figure S1. Hexagonal-shaped crystals of HheG wild type (**A**) and variants V46K (**B**), A141K (**C**), and R185K (**D**) after 72 h of crystallization.

Table S3. Crystallization kinetic parameters of different HheG variants based on the theory of Avrami of isothermal phase change.

Variant	S_{max} [mg]	k [h^{-1}]	n	$t_{0.5}$ [h]
WT	12.7	0.011	1.9	9.4
D114C	16.5	0.249	1.3	2.2
V46K	11.4	0.003	2.0	16.6
A141K	15.2	0.133	1.5	3.0

$$S = S_{max} \cdot \left(1 - e^{-k \cdot t^n}\right) \qquad \text{(Equation S1)}$$

with:

- $t_{0.5}$ = half time of crystallization process
- S = amount of crystals [mg]
- S_{max} = maximal amount of crystals [mg]
- k = velocity constant [h^{-1}]
- n = Avrami exponent [1]

$$n = a + p \cdot N_{dim} \qquad \text{(Equation S2)}$$

with:

- a = nucleation rate
- p = factor which describes control of growth
- N_{dim} = Dimensions of crystal growth [2]

Cross-linking

Table S4. Structure and spacer length of the lysine-specific cross-linkers DST, DMP, DMS, DSP and Sulfo-EGS used in this study.

Cross-linker	Cross-linker type	Spacer length [Å]
Disuccinimidyl tartrate (DST) 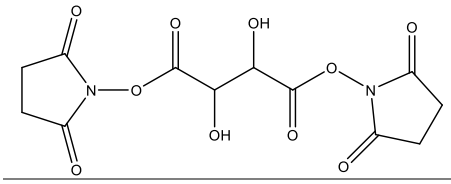	N-hydroxy-succinimid	6.4
Dimethylpimelimidate (DMP) 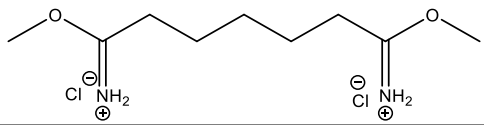	Imidoester	9.2
Dimethylsuberimidat (DMS) 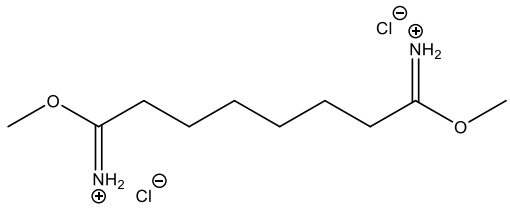	Imidoester	11.0
Dithiobis(succinimidyl)propionate (DSP) 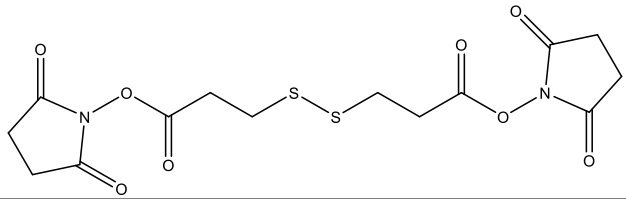	N-hydroxy-succinimid	12.0
Ethylene glycol bis(sulfosuccinimidyl succinate) (Sulfo-EGS) 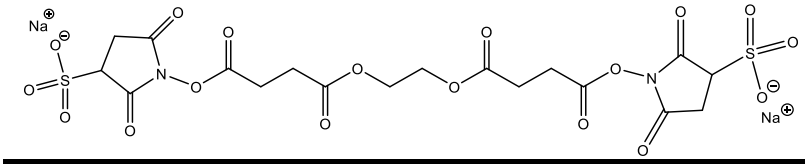	N-hydroxy-succinimid	16.1

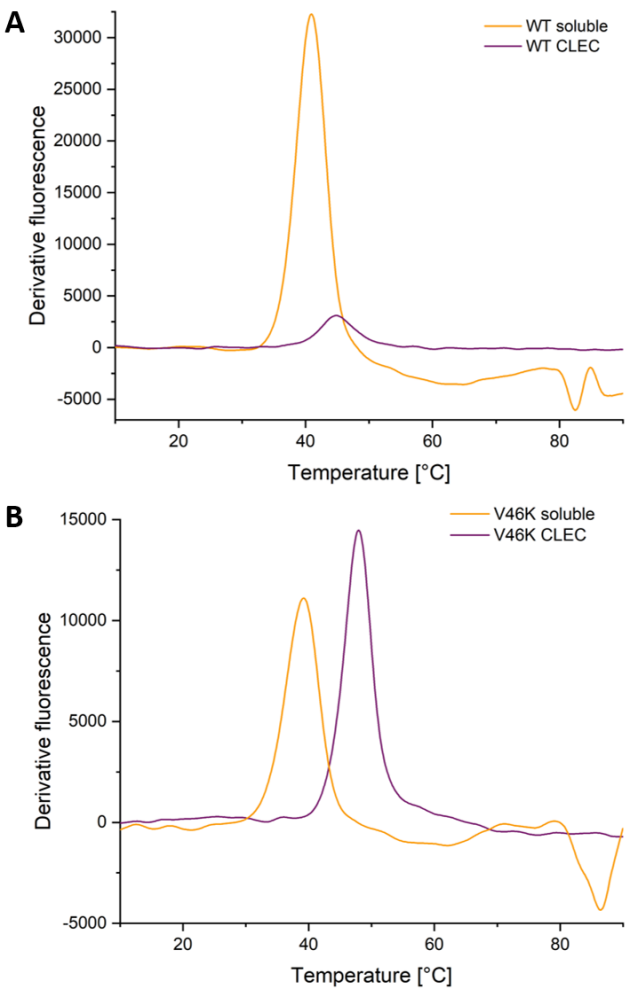

Figure S2. First derivative of the measured fluorescence signal obtained by thermal shift analysis of wild-type HheG (**A**) and variant V46K (**B**) in soluble and CLEC form. Respective CLECs were obtained after cross-linking with DSP.

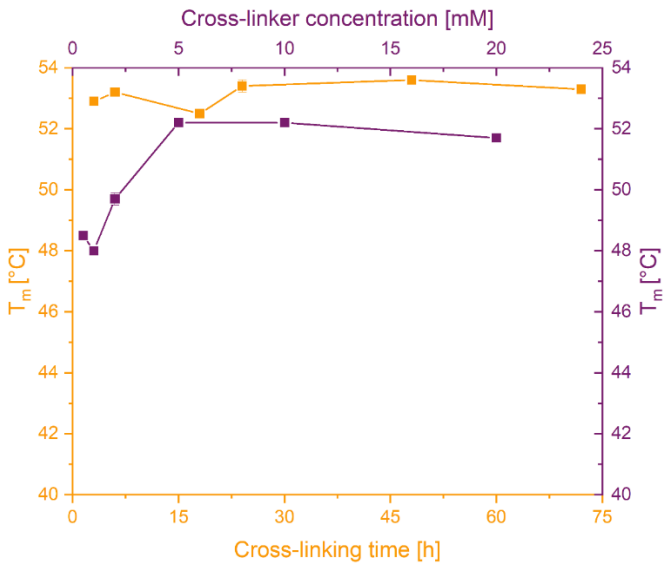

Figure S3. Dependency of apparent melting temperature (T_m) of HheG V46K CLECs (cross-linked with DSP) on cross-linker concentration (purple, fixed cross-linking time of 24 h) and cross-linking time (orange, 4 mM fixed cross-linker concentration).

Further CLEC characterization

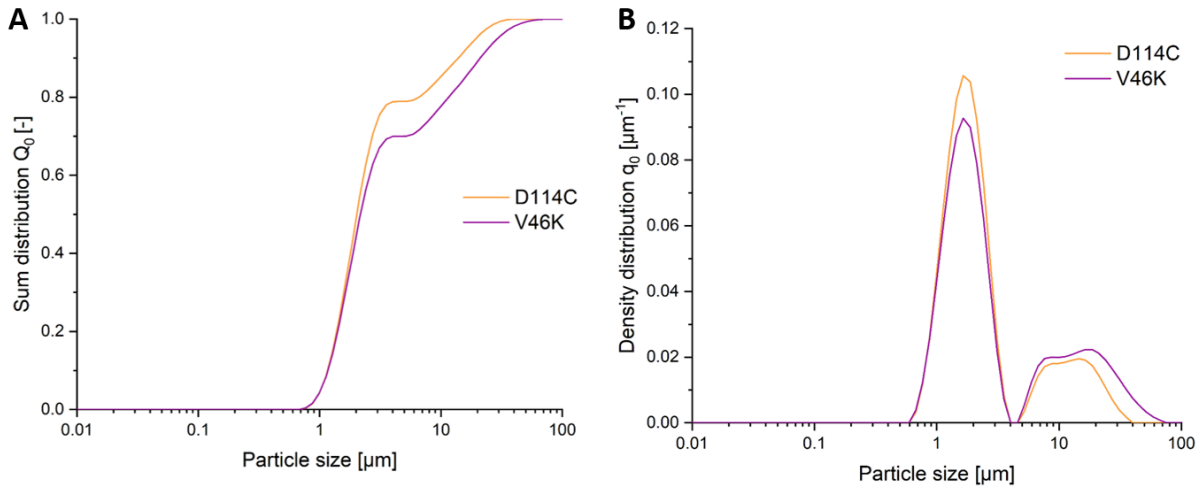

Figure S4. Particle size distribution analysis. Sum (**A**) and density distribution (**B**) are displayed for CLECs of HheG D114C (orange) and V46K (purple). Particle size analysis was performed using a Mastersizer 3000.

Table S5. Cumulative undersizes for 10, 50 and 90% of D114C and V46K CLECs.

CLEC variant	d_{10} [µm]	d_{50} [µm]	d_{90} [µm]
D114C	1.16	2.01	13.9
V46K	1.17	2.17	21.1

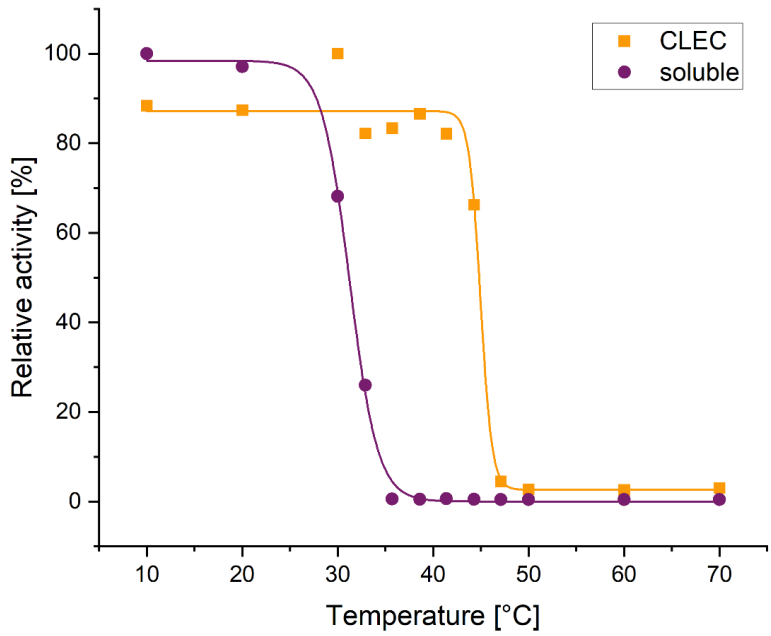

Figure S5. Thermal inactivation of HheG V46K in soluble (purple) and CLEC (orange) form. Relative activities in the conversion of 20 mM cyclohexene oxide with 40 mM azide were determined at 22°C after incubation of the enzyme preparation at respective temperatures for each 30 min.

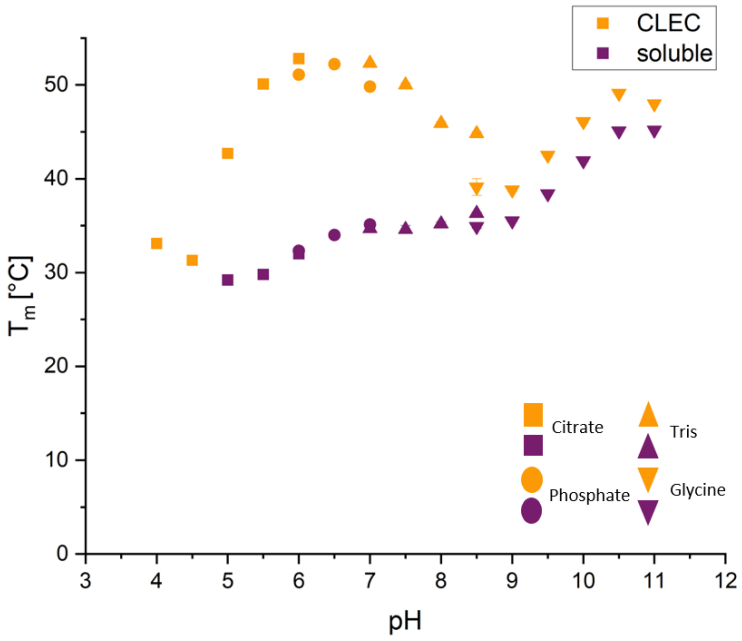

Figure S6. Melting temperature (T_m) determination of HheG V46K in soluble (purple) and CLEC (orange) form depending on pH. Measurements were performed in triplicate. At values below pH 5, protein precipitation occurred for soluble enzyme and hence, no melting temperature could be determined.

Table S6. Difference in apparent melting temperature (ΔT_m) of soluble HheG V46K and V46K CLECs in the presence and absence of 10% (v/v) co-solvent. Respective melting temperatures without co-solvent addition are 39 °C and 53.4 °C for soluble enzyme and CLECs, respectively.

Solvent	Form	$\Delta T_{m,\ \text{with solvent} - \text{without solvent}}$ [K]
DMSO	Soluble	-4
	CLEC	-0.4
DMF	Soluble	-10.4
	CLEC	-6.5
ACN	Soluble	-11.5
	CLEC	-8.2
EtOH	Soluble	-8.7
	CLEC	-8.7
iPrOH	Soluble	-9.9
	CLEC	-9.7
MeOH	Soluble	-6.9
	CLEC	-6.3

Determination of enzymatic half-life

Table S7. Experimentally determined deactivation rate constants (k_d) at the respective temperatures for HheG V46K CLECs and soluble enzyme.

Enzyme form	Temperature [K]	k_d [min^{-1}]
Soluble	303.15	0.005
	305.15	0.013
	307.15	0.025
CLEC	309.15	0.004
	311.15	0.005
	313.15	0.007

$$k_d = \frac{k_b \cdot T}{h} \cdot e^{-\frac{H-TS}{RT}} \qquad \textit{(Equation S3)}$$

$$E_d = -R \cdot T \cdot ln\left(\frac{k_d \cdot h}{k_b \cdot T}\right) \qquad \textit{(Equation S4)}$$

$$t_{1/2} = \frac{ln2}{k_d} \qquad \textit{(Equation S5)}$$

With k_b (Boltzman constant) = $1.38 \cdot 10^{-23}$ J/K and h (Planck constant) = $6.63 \cdot 10^{-34}$ J·s

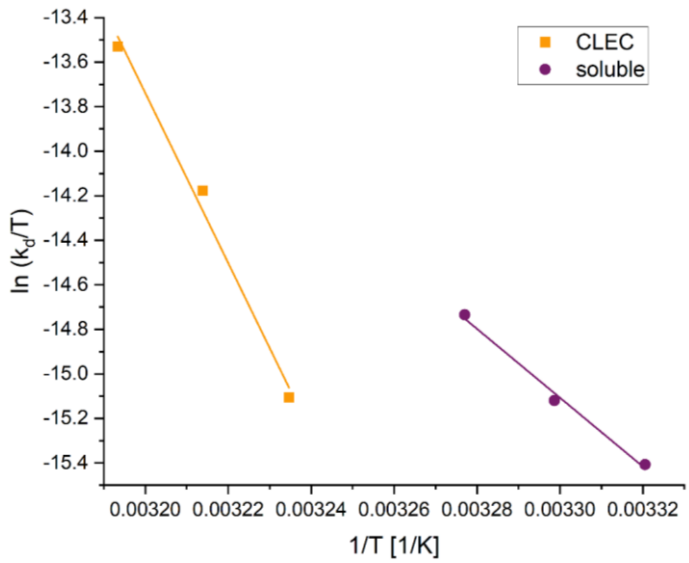

Figure S7. Eyring plot [3] of deactivation rate constants determined for HheG V46K in soluble (purple) and CLEC form (orange) at 303.15, 305.15, 307.15 K and 309.15, 311.15, 313.15 K, respectively.

Table S8. Half-life time ($t_{1/2}$) and deactivation energy (E_d) of HheG V46K CLECs and soluble enzyme at 22 °C.

Enzyme form	$t_{1/2}$	E_d [kJ/mol]
Soluble	23 h	36.5
CLEC	82 d	47.5

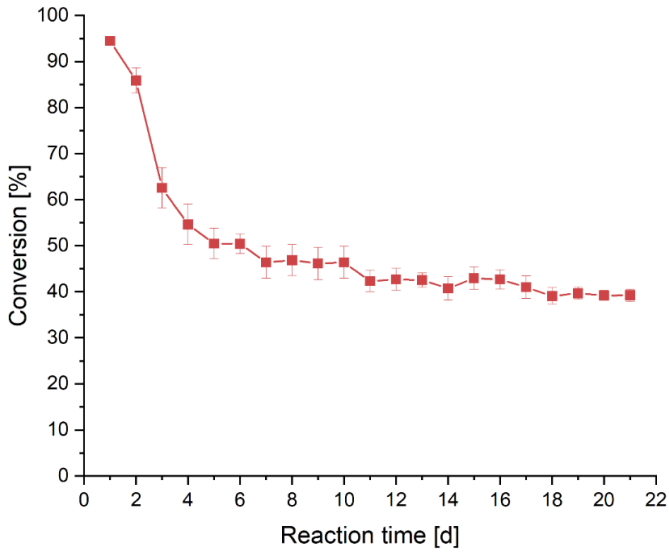

Figure S8. Repetitive batch reactions of cyclohexene oxide and azide at 22°C with reuse of HheG V46K CLECs. Each reaction cycle of 24 h contained 20 mM cyclohexene oxide, 40 mM azide and the CLECs in a total of 1 mL. For the first cycle, 100 µg of HheG V46K CLECs were applied. After 24 h of reaction, the CLECs were centrifuged, the supernatant was removed and fresh reaction media including the substrates was added to start a new cycle. Standard deviations are based on quintuple measurements. For comparison, chemical background conversion in this reaction (one cycle) without enzyme addition reached 24%.

GC analysis

To determine conversion or product enantiomeric excess of biocatalytic reactions, GC analysis (GC2010 plus, Shimadzu, Duisburg, Germany) was performed after extraction of reaction samples. Achiral separation was carried out using an OPTIMA 5 MS column (30 m length, 0.25 mm inner diameter, 0.25 µm film thickness, Macherey Nagel, Düren, Germany), whereas chiral analysis was performed using a HYDRODEX γ-DIMOM column (25 m length, 0.25 mm inner diameter, 0.25 µm film thickness, Macherey Nagel) with 40 cm/s hydrogen carrier gas flow. Temperature programs and respective retentions times for different compounds are listened in Table S9.
Conversions were determined based on the peak area of formed product devided by the combined peak areas of residual substrate and formed product.

Table S9. GC temperature programs and retention times of substrates and products used in this study [4].

Compound	Temperature program	Retention time
Achiral separation (OPTIMA 5 MS)		
cyclohexene oxide (**1**)	110 °C, 7.5 min // 50 °C/min // 295 °C	2.0 min
2-azido-1-cyclohexanol (**2a**+**2b**)		5.4 min
Chiral separation (HYDRODEX γ-DIMOM)		
cyclohexene oxide (**1**)	100°C, 40 min // 10 °C/min // 200 °C	3.1
(1*S*, 2*S*)-2-azidocyclohexan-1-ol (**2b**)		34.1 min
(1*R*, 2*R*)-2-azidocyclohexan-1-ol (**2a**)		35.4 min

References

1. Avrami, M. Kinetics of Phase Change. I General Theory. *J. Chem. Phys.* **1939**, *7*, 1103–1112, doi:10.1063/1.1750380.
2. Moreno-Cencerrado, A.; Iturri, J.; Toca-Herrera, J.L. In-Situ 2D Bacterial Crystal Growth as a Function of Protein Concentration: An Atomic Force Microscopy Study. *Microsc. Res. Tech.* **2018**, *81*, 1095–1104, doi:10.1002/jemt.23075.
3. Eyring, Henry.; Stearn, A.E. The Application of the Theory of Absolute Reacton Rates to Proteins. *Chem. Rev.* **1939**, *24*, 253–270, doi:10.1021/cr60078a005.
4. Solarczek, J.; Klünemann, T.; Brandt, F.; Schrepfer, P.; Wolter, M.; Jacob, C.R.; Blankenfeldt, W.; Schallmey, A. Position 123 of Halohydrin Dehalogenase HheG Plays an Important Role in Stability, Activity, and Enantioselectivity. *Sci. Rep.* **2019**, *9*, 1–10, doi:10.1038/s41598-019-41498-2.